Microarray Detection of Human Parainfluenzavirus 4 Infection Associated with Respiratory Failure in an Immunocompetent Adult

Charles Y. Chiu,[1,3,a] Silvi Rouskin,[1,a] Anita Koshy,[7,a] Anatoly Urisman,[1] Kael Fischer,[1] Shigeo Yagi,[8] David Schnurr,[8] Paul B. Eckburg,[7] Lucy S. Tompkins,[7] Brian G. Blackburn,[7] Jason D. Merker,[6] Bruce K. Patterson,[6,7] Don Ganem,[2,3,4,5] and Joseph L. DeRisi[1,4,5]

Departments of [1]Biochemistry and Biophysics, [2]Microbiology, [3]Infectious Diseases, and [4]Medicine and [5]Howard Hughes Medical Institute, University of California, San Francisco, [6]Department of Pathology and [7]Division of Infectious Diseases and Geographic Medicine, Department of Medicine, Stanford School of Medicine, Palo Alto, and [8]Viral and Rickettsial Disease Laboratory, California Department of Health Services, Richmond, California

A pan-viral DNA microarray, the Virochip (University of California, San Francisco), was used to detect human parainfluenzavirus 4 (HPIV-4) infection in an immunocompetent adult presenting with a life-threatening acute respiratory illness. The virus was identified in an endotracheal aspirate specimen, and the microarray results were confirmed by specific polymerase chain reaction and serological analysis for HPIV-4. Conventional clinical laboratory testing using an extensive panel of microbiological tests failed to yield a diagnosis. This case suggests that the potential severity of disease caused by HPIV-4 in adults may be greater than previously appreciated and illustrates the clinical utility of a microarray for broad-based viral pathogen screening.

Hospitalized patients who are admitted with unexplained critical respiratory illness have a high mortality rate, often >30% [1]. In the Unexplained Deaths and Critical Illnesses Project study from 1995–1998, a putative infectious agent was identified only 39% of the time, despite extensive laboratory testing [1]. Thus, there is a need for new approaches to the identification of pathogens in this setting. Here, we describe a case of human parainfluenzavirus type 4 (HPIV-4) infection in an immunocompetent adult who presented with rapidly progressive respiratory failure. Extensive conventional microbiological testing for infectious agents was unrevealing. The causative pathogen was finally identified in a sample of endotracheal aspirate using the Virochip (University of California, San Francisco), a pan-viral DNA microarray that is designed to detect both known and novel viruses on the basis of sequence homology [2, 3]. To our knowledge, this is the first report of respiratory failure from HPIV-4 in a healthy, immunocompetent adult.

CASE REPORT

A previously healthy 28-year-old woman presented to Stanford University Medical Center (Palo Alto, CA) in December 2005 with a 10-day history of fever, productive cough with hemoptysis, night sweats, and myalgia. Three days prior to admission, she was treated as an outpatient with oral azithromycin for presumptive community-acquired pneumonia, but her symptoms worsened despite treatment. The patient lived in Norway prior to moving to California in October 2005. She was a laboratory researcher but denied occupational exposure to infectious agents. She had 2 pet cats and was a cigarette smoker. A coworker had also recently been ill with a respiratory tract infection.

At admission, the patient had a temperature of 39°C and a resting oxygen saturation of 96% that decreased

Received 21 April 2006; accepted 8 June 2006; electronically published 1 September 2006.

[a] C.Y.C., S.R., and A.K. contributed equally to this article.

Reprints or correspondence: Dr. Joseph L. DeRisi, Dept. of Biochemistry and Biophysics, University of California, San Francisco at Mission Bay, Office BH403C, QB3 Bldg., 1700 4th St., San Francisco, CA 94158 (joe@derisilab.ucsf.edu).

Clinical Infectious Diseases 2006; 43:e71–6

1058-4838/2006/4308-00E1$15.00

to 80% with any movement. Her leukocyte count was 21,000 cells/mm^3, with 87% neutrophils. A chest radiograph revealed bilateral reticulonodular infiltrates (figure 1*A*), and a CT angiogram revealed diffuse bronchiolitis (figure 1*B*). The patient was treated with ceftriaxone and doxycycline and was placed in respiratory droplet isolation. The results of initial laboratory tests, including blood and sputum cultures, rheumatoid factor, and antinuclear antibody, were negative.

On day 3 after hospital admission, the patient underwent bronchoscopy, which revealed mild edema and hyperemic bronchioles. The results of an immunofluorescence test for *Pneumocystis jiroveci* were negative, as were bacterial, fungal, and acid-fast bacilli cultures of bronchoalveolar lavage fluid samples. A shell vial assay for cytomegalovirus and cytomegalovirus PCR of bronchoalveolar lavage fluid specimens also yielded negative results. Direct fluorescent antibody testing of bronchoalveolar lavage fluid using the D^{3TM}-DFA Respiratory Virus Screening and ID Kit (Diagnostic Hybrids) failed to detect respiratory syncytial virus, adenovirus, influenzavirus A and B, and parainfluenzavirus types 1, 2, and 3. Likewise, viral bronchoalveolar lavage fluid culture using 2 rhesus monkey kidney cell lines, 2 human fibroblast cell lines, and a continuous A549 human alveolar epithelial cell line failed to demonstrate cytopathic effect or hemadsorption, despite incubation for 21 days. After bronchoscopy, the patient became dependent on mechanical ventilation and pressors, and serial chest radiographs revealed persistent bilateral infiltrates (figure 1*C*). Antimicrobial therapy was changed to moxifloxacin and oseltamivir, and high-dose methylprednisolone therapy was initiated. Results of viral direct fluorescent antibody testing for the 7 respiratory viruses and 14-day viral cultures performed on endotracheal aspirate specimens obtained on days 3 and 4 after hospital admission were negative. Nose swab viral cultures performed on day 5 were also negative.

On day 7 after hospital admission, given her critically ill condition and persistent unexplained respiratory failure, the patient underwent a diagnostic open-lung biopsy. Histopathologic analysis revealed an organizing bronchiolitis without granulomas, multinucleated giant cells, or viral nuclear inclusions (figure 1*D*). The pathology was primarily bronchiolocen-

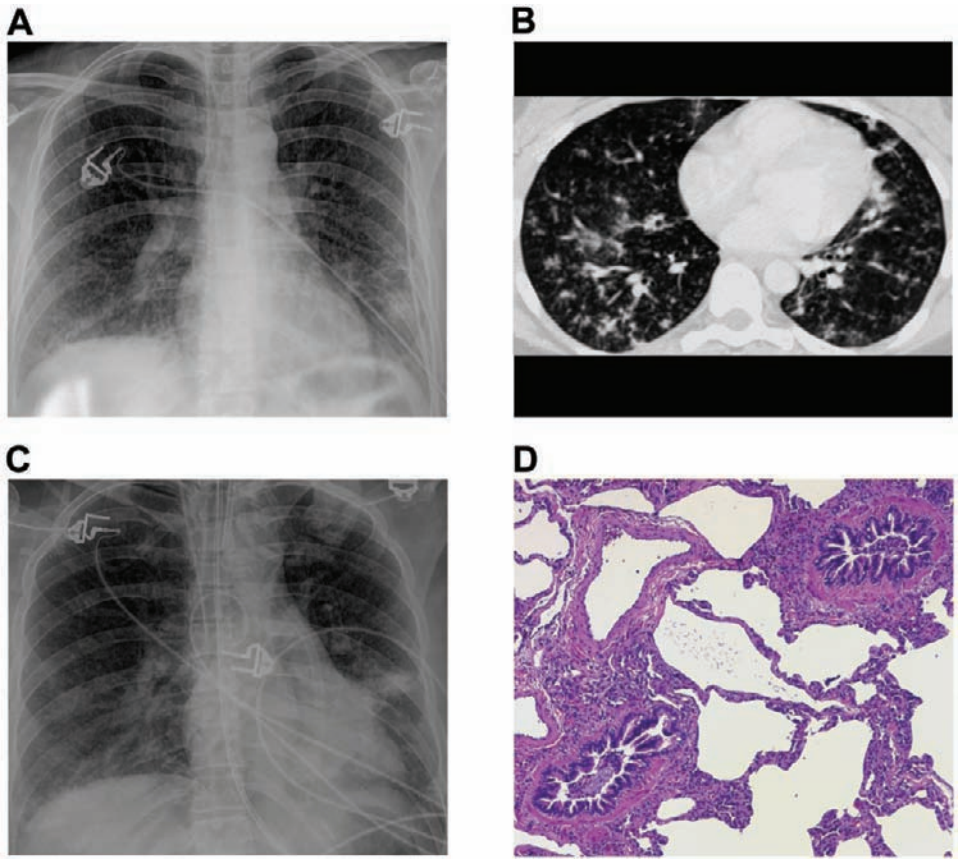

Figure 1. Imaging and lung pathology from the patient. A chest radiograph *(A)* obtained at admission revealed bilateral reticulonodular infiltrates with associated lower lobe consolidations, whereas a CT scan (representative slice; *B)* showed bilateral centrilobular nodules with a tree-in-bud appearance suggestive of bronchiolitis. After intubation, a chest radiograph was performed on the patient on hospital day 4 that revealed persistent bilateral infiltrates *(C).* On day 7 after hospital admission, findings from lung biopsy analysis revealed an organizing bronchiolitis but no direct histological evidence of virus infection (hematoxylin and eosin stain, low magnification; *D).*

tric, with the lumens of the bronchioles filled with granulation tissue plugs and eosinophils. These features were not typical for vasculitis, cryptogenic organizing pneumonia, or acute bronchopneumonia.

The patient improved clinically with continued supportive care, and by day 15 after hospital admission, she was weaned off of mechanical ventilation. She was discharged on day 26 after hospital admission. Additional laboratory studies performed during the course of the patient's hospitalization failed to identify the etiology of her illness. These studies included PCR of brochoalveolar lavage fluid specimens for the severe acute respiratory syndrome (SARS) coronavirus and for metapneumovirus, as well as PCR and direct fluorescent antibody testing of a nasopharyngeal specimen for *Bordetella pertussis*. A urine test for *Legionella* antigen and a serum test for cryptococcal antigen both yielded negative results. Results of serological analyses for HIV infection, histoplasmosis, blastomycosis, tularemia, sporotrichosis, Q fever, leptospirosis, and Sin Nombre hantavirus infection were negative. Serum samples were tested twice during the patient's hospitalization for coccidioidomycosis, *Mycoplasma* and *Chlamydia* antibodies, and the results were also negative.

Ultimately, diagnosis was made by examination of an endotracheal aspirate from hospital day 4 using the Virochip assay. The findings on microarray indicated the presence of HPIV-4, which was confirmed by subsequent specific PCR and serological analysis.

METHODS

Clinical specimen collection and microarray screening. On day 4 after hospital admission, an endotracheal aspirate specimen from the patient was collected in a sterile cup containing a viral culture medium (MEM [Nissui Corporation]) and stored at −80°C. The sample used in the study was obtained according to protocols approved by Stanford University's Institutional Review Board. Total RNA obtained from 1 mL of sample was extracted using RNA-Bee (IsoTex Diagnostics), reverse-transcribed to cDNA, amplified by a modified Round A/B random PCR method, and hybridized to the Virochip as previously described [2–4]. The Virochip was scanned with an Axon 4000B scanner (Axon Instruments) and GenePix software, version 3.0 (NCBI GEO, series GSE4191).

The third-generation Virochip used here (NCBI GEO, platform GPL3429; ~22,000 oligonucleotides) was designed using all partial sequences and fully-sequenced genomes deposited in the GenBank database as of June 2004 (~277,000 sequences) and is a major expansion of the previous second-generation chip (~11,000 oligonucleotides) [3], which was designed in 2002 using fully-sequenced reference genomes (~1000 sequences). Importantly for this study, the new microarray design incorporates partial sequence information from 16 paramyxoviridae species for which complete genomic sequences are not available.

Microarray analysis was performed by ranking the highest intensity viral oligonucleotides by *z*-score. The *z*-score for a specific oligonucleotide is defined as the distance in SDs of the oligonucleotide intensity from its median intensity across all arrays in our database performed to date ($n = 1083$).

Microarray confirmation with PCR and serological analysis. Microarray evidence of HPIV-4 was confirmed by PCR of amplified cDNA from the patient's endotracheal aspirate followed by sequencing. Previously published primers [5–8] were used to amplify segments of the HPIV-4 genome corresponding to the nucleoprotein, phosphoprotein, and matrix genes. New primer sets were also designed to amplify conserved regions within the genes coding for the fusion protein (RUBULA-F1: 5′-TTGCWGGDGTDGYKRTWGG-3′; RUBULA-R1: 5′-TTTGCWGGDGTDGYKRTWGG-3′) and large protein (PI2-F1: 5′-GAGTAATGAGCATGGTTCAAGGAG-3′; PI2-R1: 5′-CAGGAAGCTTGAGTACATTCACCTA-3′). The RUBULA-F1 and RUBULA-R1 degenerate primers were derived from ClustalW sequence alignment of the fusion genes from parainfluenza 4a, parainfluenza 4b, and mumps viruses, whereas the PI2-F1 and PI2-R1 primers were derived from the sequence of the HPIV-2 large protein gene. Each reaction contained 5.0 μL of 10× PCR buffer (Invitrogen Corporation), 2.0 μL of 50 mmol/L $MgCl_2$, 1.0 μL of 10 mmol/L deoxyribonucleoside triphosphates, 1.0 μL of forward primer and 1.0 μL of reverse primer (10 pmol/μL each), 1 μL of Platinum Taq DNA polymerase (Invitrogen Corporation; 5 U/μL), and 5.0 μL of template cDNA. Cycling parameters were as follows: 5 min of initial denaturation at 94°C followed by 40 cycles of denaturation (30 s at 94°C), annealing (45 s at 50°C), and elongation (60 s at 72°C), with a final extension at 72°C for 8 min. Appropriate positive and negative controls were included with each reaction, and amplified PCR bands of the expected size were sequenced on an ABI PRISM 3700 DNA Analyzer (Applied Biosystems). Sequences were then compared with HPIV-4 entries in the GenBank database using the BLAST algorithm [9].

Specific serological analysis for HPIV-4 using an indirect immunofluorescence assay was performed according to established protocols as previously reported [10]. Slides prepared from primary monkey kidney cells that were productively infected with human parainfluenzavirus 4a were used for the immunofluorescence assay.

Broad-range PCR of lung biopsy tissue. DNA was extracted from fresh-frozen lung tissue using the QIAamp DNA Mini Kit (Qiagen). Broad-range bacterial 16S and fungal 18S rDNA PCR was performed on extracted DNA using bacterial primers 8F (5′-AGAGTTTGATCCTGGCTCAG-3′) and 806R (5′-GGACTACCAGGGTATCTAAT-3′) and fungal primers

ITS1-F (5′-CTTGGTCATTTAGAGGAAGTAA-3′) and ITS1-4R (5′-TCCTCCGCTTATTGATATGC-3′) [1, 11, 12]. Each reaction contained 5.0 μL of 10× PCR buffer-II (Applied Biosystems), 3.0 μL of 25 mmol/L $MgCl_2$, 2.5 μL of 1% Triton X-100, 4.0 μL of 250 mmol/L tetramethylammonium chloride, 2.0 μL of 10 mmol/L deoxyribonucleoside triphosphates, 1.0 μL of forward primer and 1.0 μL of reverse primer (20 pmol/μL each), 0.5 μL of AmpliTaq DNA polymerase (Applied Biosystems; 5 U/μL), and 5.0 μL of template DNA. Cycling parameters were as follows: 5 min of initial denaturation at 95°C, followed by 35 cycles of denaturation (30 s at 95°C), annealing (30 s at 56°C), and elongation (60 s at 72°C), with a final extension at 72°C for 8 min. A mock extraction control was included throughout the tissue lysis and PCR. Amplified products were verified by gel electrophoresis using 1.0% agarose gels.

RESULTS

Because conventional diagnostic test results were negative, the Virochip, a pan-viral DNA microarray, was used to screen for a possible infectious agent. Traditional methods of microarray analysis include visual inspection and hierarchical clustering [13, 14]. Visual inspection involves examination of the viral identities of the oligonucleotides with the highest intensities, whereas hierarchical clustering uses a set of microarrays to group oligonucleotides with similar intensity profiles to identify patterns that may correspond to a particular virus. Neither visual inspection nor hierarchical clustering detected a convincing viral signature on the microarray. Thus, we used a new data analysis method, the *z*-score metric, which has been implemented in our laboratory for identifying weak viral signatures. The *z*-score metric estimates the statistical significance of individual oligonucleotides on the microarray. Manual inspection of the top 100 viral oligonucleotides ranked by *z*-score revealed a possible paramyxovirus signature, because 6 paramyxoviridae oligonucleotides were among the top 100 with *z*-scores ranging from 2.21–3.71 (figure 2*B*, 1–6). Four of the oligonucleotides were derived from human parainfluenzavirus 4a, 1 from human parainfluenzavirus 4b, and 1 from simian parainfluenzavirus 5, a close relative of HPIV-4. The 6 oligonucleotides mapped to 4 different regions in the HPIV-4 genome, corresponding to the nucleocapsid protein, phosphoprotein, fusion protein, and large protein (figure 2*A* and 2*B*).

The microarray finding of HPIV-4 was then confirmed by PCR of amplified cDNA obtained from the patient's endotracheal aspirate specimen. PCR using primers directed to the fusion gene of HPIV-4 yielded a 473–base pair fragment that was sequenced and found to share 97% nucleotide identity and 99% amino acid identity with the corresponding region of HPIV-4a in the GenBank database (figure 2*C*, d). HPIV-4 sequences from the nucleoprotein, phosphoprotein, matrix, and large protein genes were also obtained by PCR (figure 2*C*, a–e). All fragments shared over 92% nucleotide identity with available HPIV-4 sequences in the GenBank database, including 99% nucleotide identity in the matrix protein—the most conserved region of the HPIV-4 genome (figure 2*C*, c).

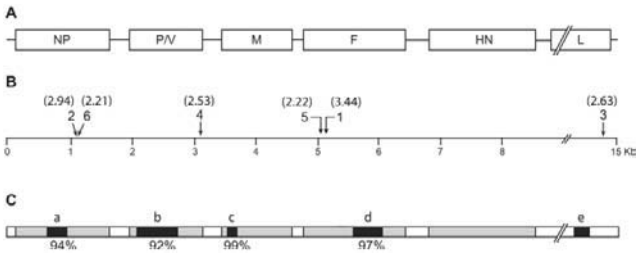

Figure 2. Graphic representation of the human parainfluenzavirus 4 (HPIV-4) genome *(A)*. The major viral proteins include the nucleocapsid protein (NP), phosphoprotein (P), nonstructural V protein (V), matrix protein (M), fusion protein (F), hemagglutinin-neuraminidase protein (HN), and large protein (L). The locations of the 6 paramyxovirus oligonucleotides used to detect HPIV-4 on the microarray are mapped onto the ~15 kB genome *(B)*. The corresponding *z*-score for each oligonucleotide is indicated in parentheses. Five regions of the HPIV-4 virus obtained from a sample of the patient's endotracheal aspirate were sequenced *(a–e, black areas)*, 4 of which are within previously sequenced regions of the genome *(gray areas; C)*. Below each sequenced region is its percentage of nucleotide identity to the corresponding HPIV-4a sequence in the GenBank database.

The diagnosis of HPIV-4 infection was confirmed by examining antibody titers from patient serum samples that were collected on days 13, 23, 24, 31, and 51 after symptom onset, using an indirect immunofluorescence assay (figures 3*A* and 3*B*). A specific antibody response against HPIV-4 was observed, with an 8-fold increase in IgG from day 13 (1:128) to day 24 (1:1024). The HPIV-4–specific IgG titers remained elevated >7 weeks after symptom onset during the patient's convalescent phase. In contrast, the results of convalescent-phase serological analysis for parainfluenzavirus types 1, 2, and 3 performed at 7 weeks were negative, with IgG antibody titers of <1:8 by complement fixation. Broad-range PCR of extracted lung biopsy DNA using universal bacterial and fungal primers was also negative.

DISCUSSION

We report a case of HPIV-4 infection in a previously healthy adult who presented with a life-threatening febrile respiratory illness. The key to identifying HPIV-4 was examining a broader range of viral pathogens than is typical of standard clinical laboratories. The Virochip is particularly well-suited for this purpose, because it allows the unbiased detection of genomes from all known viral families in a single assay. Although the

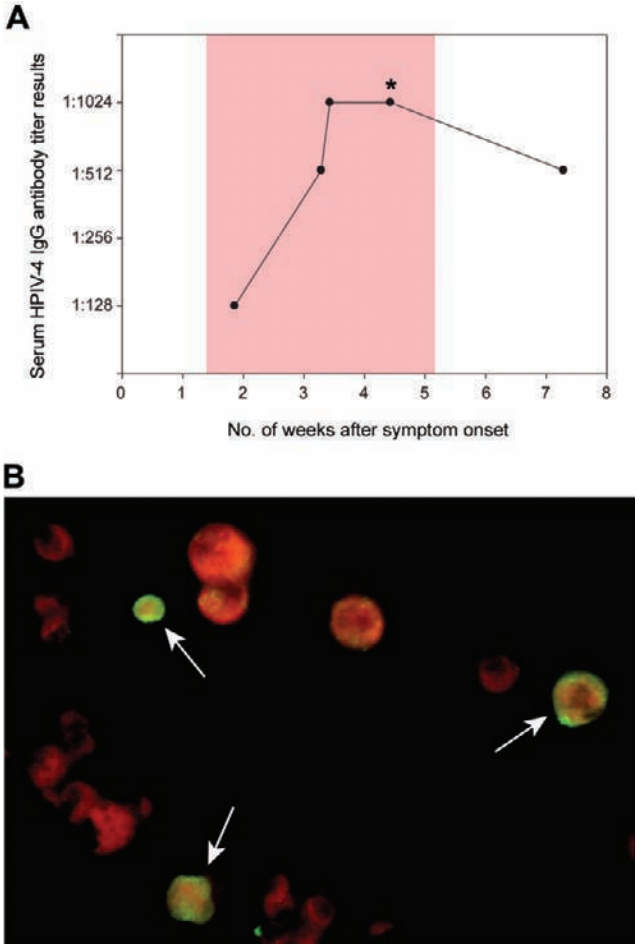

Figure 3. Detection of antibody to human parainfluenzavirus 4 (HPIV-4) by indirect immunofluorescence. *A,* Plot of the patient's serum HPIV-4 IgG antibody titers over time. The 5 successive time points correspond to days 13, 23, 24, 31, and 51 after symptom onset, the pink background outlines the period of hospitalization, and the asterisk designates the time point corresponding to panel B. The cytoplasm of infected cells *(white arrows)* stains green against a background of uninfected cells in red *(B).*

Virochip is an experimental research tool, a potential application of this new technology, as demonstrated here, is rapid and comprehensive screening for putative viral pathogens in the acute clinical setting.

Because the patient was already receiving antibiotics at the time of admission, negative culture results did not rule out a concomitant bacterial or fungal infection. However, our negative results from broad-range PCR of lung biopsy DNA using universal bacterial and fungal primers argued against this possibility. Furthermore, the overall clinical picture of a virus-like upper respiratory infection prodrome, bilateral reticulonodular pulmonary infiltrates, bronchiolitis on bronchoscopy, and steady disease progression despite administration of broad-spectrum antibiotics is most consistent with severe viral bronchiolitis/pneumonitis, and not with bacterial pneumonia.

HPIV-4 was identified as a potential candidate pathogen by microarray and subsequent PCR of an endotracheal aspirate sample collected on day 4 after hospital admission. Longitudinal studies in children suggest that human parainfluenzaviruses can be shed from the oropharynx for as long as 3–4 weeks [15]. Thus, it is not surprising that we were still able to detect HPIV-4 from a specimen collected on day 4 after hospital admission (which corresponds to ~14 days after symptom onset). Nosocomial infection with HPIV-4 is a remote possibility, although a study of patients who received a diagnosis of acute viral pneumonia in the intensive care unit revealed that nearly all of these illnesses (11 [92%] of 12) were community acquired [16]. Moreover, the patient's HPIV-4–specific IgG antibody titer was already elevated at 1:128 by day 3 after hospital admission, making a nosocomial infection with HPIV-4 extremely unlikely. Despite extensive microbiological testing, no other pathogen was identified in the patient's case. The documented seroconversion that accompanied the clinical infection provides strong additional support that this virus is the etiologic agent for the patient's illness.

HPIV-4 has primarily been associated with mild upper respiratory infections in children and adults. Although serological evidence suggests that HPIV-4 may account for up to 3% of all respiratory tract infections [17], the clinical significance of HPIV-4 in immunocompetent individuals is unknown. Diagnosis of HPIV-4 infection is problematic because HPIV-4 is difficult to isolate in viral cultures, and standard commercial direct fluorescent antibody panels available in most clinical virology laboratories include only HPIV-1, -2, and -3 [18]. In rare instances, HPIV-4 has been shown to cause severe respiratory disease in children [17–19] and immunocompromised individuals [20], but hitherto, it has not been associated with acute respiratory failure in healthy, young adults. This case further expands the documented clinical spectrum of HPIV-4 infection and supports specific testing for HPIV-4 in individuals with unexplained critical respiratory illness.

Acknowledgments

We thank Elaine Yeh and Chao Pan for their help with the immunofluorescence assay and Matthew Burtelow for assistance with pathology photography. We thank Seth Bechis for PCR primer design. We thank Amy Kistler, Suzanne Noble, Dylan Pillai, and Patrick Tang for helpful discussions and comments. We also thank David A. Relman and the pathogen discovery group (Harold Amogan, Elisabeth M. Bik, and Dan B. DiGiulio, P.B.E.) of the Palo Alto Veterans Affairs Health Care System (Palo Alto, CA), for optimizing molecular methodology and providing intellectual input.

Financial support. Howard Hughes Medical Institute and Doris Duke Charitable Foundation (D.G. and J.L.D) and University of California San Francisco National Institutes of Health Infectious Diseases Training Grant (T32-AI07641; to C.Y.C.).

Potential conflicts of interest. All authors: no conflicts.

References

1. Hajjeh RA, Relman D, Cieslak PR, et al. Surveillance for unexplained deaths and critical illnesses due to possibly infectious causes, United States, 1995–1998. Emerg Infect Dis **2002**; 8:145–53.
2. Wang D, Coscoy L, Zylberberg M, et al. Microarray-based detection and genotyping of viral pathogens. Proc Natl Acad Sci U S A **2002**; 99:15687–92.
3. Wang D, Urisman A, Liu YT, et al. Viral discovery and sequence recovery using DNA microarrays. PLoS Biol **2003**; 1:E2.
4. Urisman A, Molinaro RJ, Fischer N, et al. Identification of a novel gammaretrovirus in prostate tumors of patients homozygous for R462Q RNASEL variant. PLoS Pathog **2006**; 2:e25.
5. Billaud G, Morfin F, Vabret A, et al. Human parainfluenza virus type 4 infections: a report of 20 cases from 1998 to 2002. J Clin Virol **2005**; 34:48–51.
6. Kondo K, Bando H, Kawano M, et al. Sequencing analyses and comparison of parainfluenza virus type 4A and 4B NP protein genes. Virology **1990**; 174:1–8.
7. Kondo K, Fujii M, Nakamura T, et al. Sequence characterization of the matrix protein genes of parainfluenza virus types 4A and 4B. J Gen Virol **1991**; 72:2283–7.
8. Rubinas TC, Carey RB, Kampert MC, Alkan S, Lednicky JA. Fatal hemorrhagic pneumonia concomitant with *Chlamydia pneumoniae* and parainfluenza virus 4 infection. Arch Pathol Lab Med **2004**; 128:640–4.
9. Altschul SF, Gish W, Miller W, Myers EW, Lipman DJ. Basic local alignment search tool. J Mol Biol **1990**; 215:403–10.
10. Gallo D, Hoffman MN, Yeh ET, George JR, Hanson CV. Comparison of indirect immunofluorescence and membrane fluorescence assays for the differentiation of antibodies to human immunodeficiency virus types 1 and 2. J Clin Microbiol **1992**; 30:2275–8.
11. Edwards U, Rogall T, Blocker H, Emde M, Bottger EC. Isolation and direct complete nucleotide determination of entire genes: characterization of a gene coding for 16S ribosomal RNA. Nucleic Acids Res **1989**; 17:7843–53.
12. White TJ, Bruns T, Lee S, Taylor JW. Amplification and direct sequencing of fungal ribosomal RNA genes for phylogenetics. In: Innis MA, Gelfand DH, Sninsky JJ, White TJ, eds. PCR protocols: a guide to methods and applications. New York: Academic Press, **1990**:315–22.
13. Eisen MB, Spellman PT, Brown PO, Botstein D. Cluster analysis and display of genome-wide expression patterns. Proc Natl Acad Sci U S A **1998**; 95:14863–8.
14. Urisman A, Fischer KF, Chiu CY, et al. E-Predict: a computational strategy for species identification based on observed DNA microarray hybridization patterns. Genome Biol **2005**; 6:R78.
15. Frank AL, Taber LH, Wells CR, Wells JM, Glezen WP, Paredes A. Patterns of shedding of myxoviruses and paramyxoviruses in children. J Infect Dis **1981**; 144:433–41.
16. Legoff J, Guerot E, Ndjoyi-Mbiguino A, et al. High prevalence of respiratory viral infections in patients hospitalized in an intensive care unit for acute respiratory infections as detected by nucleic acid-based assays. J Clin Microbiol **2005**; 43:455–7.
17. Rubin EE, Quennec P, McDonald JC. Infections due to parainfluenza virus type 4 in children. Clin Infect Dis **1993**; 17:998–1002.
18. Lau SK, To WK, Tse PW, et al. Human parainfluenza virus 4 outbreak and the role of diagnostic tests. J Clin Microbiol **2005**; 43:4515–21.
19. Lindquist SW, Darnule A, Istas A, Demmler GJ. Parainfluenza virus type 4 infections in pediatric patients. Pediatr Infect Dis J **1997**; 16: 34–8.
20. Miall F, Rye A, Fraser M, Hunter A, Snowden JA. Human parainfluenza type 4 infection: a case report highlighting pathogenicity and difficulties in rapid diagnosis in the post-transplant setting. Bone Marrow Transplant **2002**; 29:541–2.